BRCA1 Supports XIST RNA Concentration on the Inactive X Chromosome

Shridar Ganesan,[1] Daniel P. Silver,[1]
Roger A. Greenberg,[1] Dror Avni,[1] Ronny Drapkin,[1]
Alexander Miron,[1] Samuel C. Mok,[2]
Voahangy Randrianarison,[3] Steven Brodie,[4]
Jennifer Salstrom,[5] Theodore P. Rasmussen,[6]
Ann Klimke,[1] Christine Marrese,[1]
York Marahrens,[5] Chu-Xia Deng,[4]
Jean Feunteun,[3] and David M. Livingston[1,7]
[1]The Dana-Farber Cancer Institute
Harvard Medical School
Boston, Massachusetts 02115
[2]Laboratory of Gynecologic Oncology
Department of Obstetrics, Gynecology,
  and Reproductive Biology
Brigham and Women's Hospital
Boston, Massachusetts 02115
[3]Laboratoire de Genetique Oncologique
Laboratoire de Vectorologie et Transfert de Gènes
Institut Gustave-Roussy
Villejuif 94805
France
[4]Genetics of Development and Disease,
  Branch 10/9N105
National Institute of Diabetes, Digestive, and Kidney
  Diseases
National Institutes of Health
Bethesda, Maryland 20892
[5]Department of Human Genetics
Gonda Center
University of California, Los Angeles
Los Angeles, California 90095
[6]Center for Regenerative Biology and Department
  of Animal Sciences
University of Connecticut
Storrs, Connecticut 06269

Summary

BRCA1, a breast and ovarian tumor suppressor, colocalizes with markers of the inactive X chromosome (Xi) on Xi in female somatic cells and associates with XIST RNA, as detected by chromatin immunoprecipitation. Breast and ovarian carcinoma cells lacking BRCA1 show evidence of defects in Xi chromatin structure. Reconstitution of BRCA1-deficient cells with wt BRCA1 led to the appearance of focal XIST RNA staining without altering XIST abundance. Inhibiting BRCA1 synthesis in a suitable reporter line led to increased expression of an otherwise silenced Xi-located GFP transgene. These observations suggest that loss of BRCA1 in female cells may lead to Xi perturbation and destabilization of its silenced state.

Introduction

Women harboring a mutation in one allele of the BRCA1 gene have a significantly increased lifetime risk of breast

[7]Correspondence: david_livingston@dfci.harvard.edu

and ovarian cancer. Since tumors that arise in these individuals reveal loss of heterozygosity at BRCA1 with retention of the mutant allele, this gene is considered a tumor suppressor. It encodes an 1863 residue nuclear protein that is widely expressed and likely plays a role in several fundamental processes, including the maintenance of genomic integrity, transcription regulation, and cell cycle/checkpoint control (Deng and Brodie, 2000; Scully and Livingston, 2000; Venkitaraman, 2002).
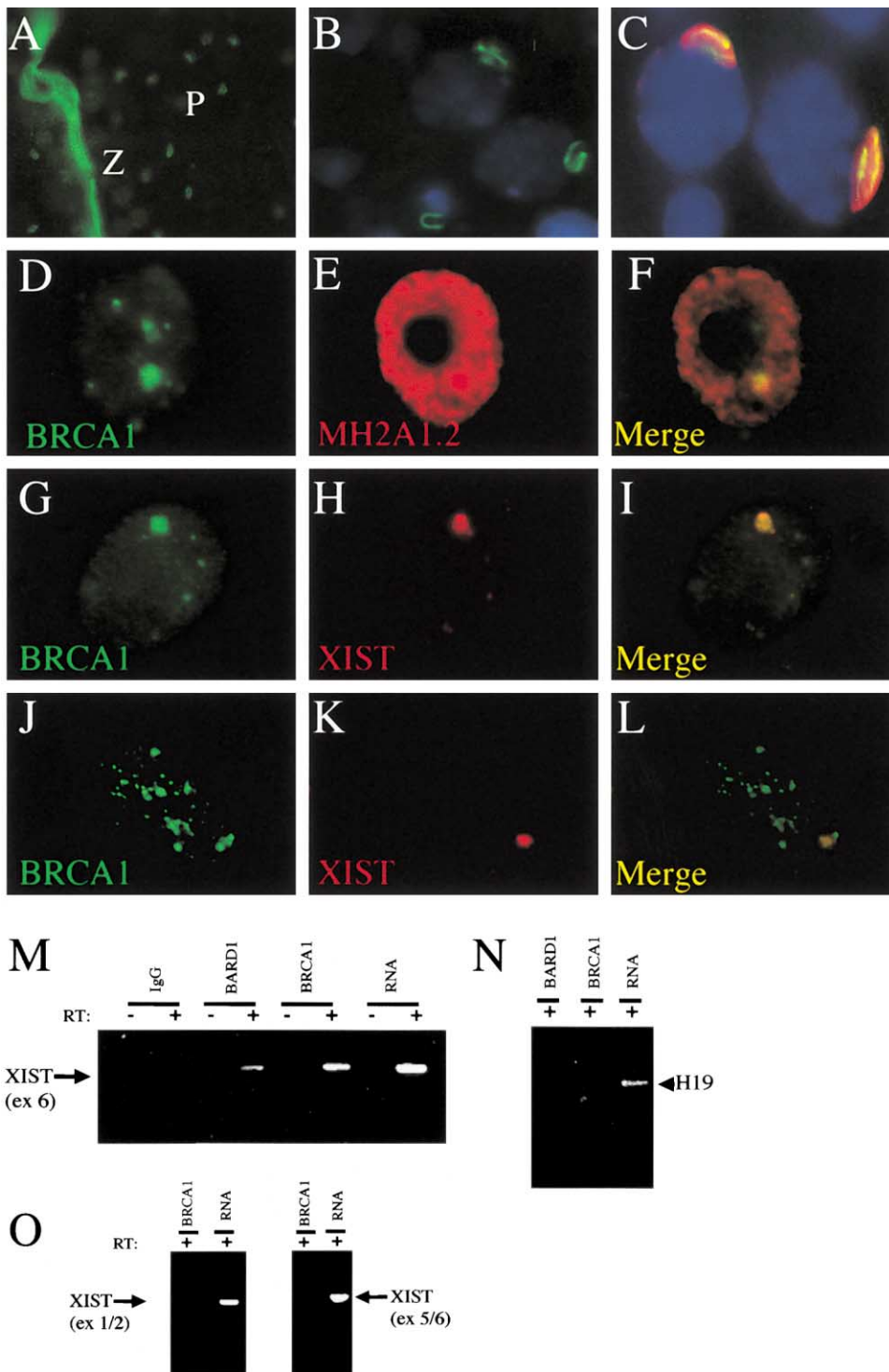
BRCA1$^{-/-}$ mouse embryos exhibit early embryonic lethality, genetic instability, and proliferation arrest (reviewed in Brodie and Deng, 2001). Cell lines lacking wt BRCA1 manifest deficits in DNA repair and homologous recombination that are complemented by the reexpression of the intact protein (Gowen et al., 1998; Moynahan et al., 1999; Scully et al., 1999). BRCA1 interacts with multiple DNA repair/recombination proteins, including Rad51, the Rad50/MRE11/Nibrin complex, Bloom's helicase, and the Fanconi D2 protein (Garcia-Higuera et al., 2001; Scully et al., 1997; Wang et al., 2000; Zhong et al., 1999). BRCA1 also interacts directly with BACH1, a DEAH helicase; this interaction appears to be essential for efficient DNA double-strand break repair (DSBR) (Cantor et al., 2001). BACH1, itself, may be a tumor suppressor (Cantor et al., 2001), suggesting a link between BRCA1/BACH1-mediated DSBR and their actions as tumor suppressors.

BRCA1 has also been implicated in transcriptional regulation, chromatin remodeling, and G2/M checkpoint control. It can interact, directly or indirectly, with multiple partners, including CTIP, ZBRK, p300, estrogen receptor (ER), HDAC, Rb, p53, RNA polymerase II holoenzyme, cyclin D1, c-*myc*, and at least one Swi/Snf complex (Bochar et al., 2000; Deng and Brodie, 2000; Zheng et al., 2000). Moreover, BRCA1 can bind directly to certain DNA structures in vitro (Paull et al., 2001). Its RING domain and that of its structurally related binding partner, BARD1, exhibit in vitro E3 ubiquitin ligase activity following complex formation (Hashizume et al., 2001). The role of these interactions in BRCA1-dependent tumor suppression is poorly understood.

The specific molecular mechanism underlying the gender and tissue specificity of the BRCA1 cancer syndrome in humans, while potentially linked to the activities noted above, remains unclear. The breast and ovary are both estrogen-responsive organs, and BRCA1 has been reported to interact with the estrogen receptor (ER) and to influence both ligand-dependent and -independent ER activation (Fan et al., 2001; Zheng et al., 2001). In addition, there may be a role for BRCA1 in breast development (Xu et al., 1999). The extent to which these properties underlie its gender- and tissue-specific tumor suppression mechanism is unknown.

BRCA1 mRNA is highly expressed in the testis (Blackshear et al., 1998). In analyzing mouse testis, we noted that BRCA1 is heavily concentrated on the X chromosome in pachytene spermatocytes. The X chromosome in these cells is transcriptionally inactive, having undergone changes reminiscent of X chromosome inactivation in female somatic cells (Richler et al., 1992). This

Figure 1. Association of BRCA1 and Markers of the Inactive X Chromosome

(A–C) Immunostaining for BRCA1 was performed on sections of mouse testis. Low-power view of testis stained for BRCA1 (FITC). The bright autofluorescent structure is the boundary of a spermatic tubule. Regions of zygotene (Z) and pachytene (P) spermatocytes are marked. (B) Close-up view of BRCA1 immunostaining of pachytene cells; DAPI nuclear staining is shown in blue; (C) pachytene cells coimmunostained for BRCA1 (green) and macrohistone H2A1 (MH2A1, red). Areas of staining overlap are shown in yellow; DAPI nuclear staining in blue.

(D–L) Combined immunostaining of telomerase-immortalized human mammary epithelial cells (D–F) with a monoclonal antibody to BRCA1 (D) and a polyclonal antibody to MH2A1 (E). Merged image (F). (G–L) depict combined immunostaining of HMEC-t (G–I) and WI-38 cells (J–L) for BRCA1 (G and J) and RNA FISH for XIST (H and K). Merged images (I and L).

(M) ChIP (see Experimental Procedures) was performed on 293 cells using purified antibodies to BRCA1, BARD1, and an irrelevant antibody. RNA was extracted from each ChIP and subjected to RT-PCR using primers specific for a region in exon 6 of XIST. The plus and minus signify PCR amplification with and without first round RT. The last two lanes are controls using cellular RNA as template.

Table 1. Colocalization of BRCA1 with XIST and Macrohistone H2A1

Cell Type	% XIST (+)	% BRCA1 (+)	% of BRCA1(+) Cells that Exhibit Colocalization of BRCA1 and XIST
HMEC-t	93	72	5.0
WI-38	95	54	10
IMR-90	96	48	8.5

Cell Type	% MH2A1 (+)	% BRCA1 (+)	% of BRCA1(+) Cells that Exhibit Colocalization of BRCA1 and MH2A1
HMEC-t	23	78	3.7
WI-38	41	52	8.0
Ishikawa	11	67	12

In experiments performed on HMEC-t, (telomerase-immortalized primary human mammary epithelial cells), WI-38, Ishikawa, and IMR90 cells, 200–300 cells of each asynchronous culture were analyzed for BRCA1 and XIST, focal MH2A1 and XIST costaining, and focal BRCA1 and MH2A1 costaining. In all instances, colocalization refers to costaining of a single, large, discrete nuclear body.

observation prompted the question of whether the BRCA1 interacts with the inactive X chromosome in female somatic cells.

Results

Colocalization of BRCA1 with the Inactive X Chromosome in Spermatocytes and Female Somatic Cells

BRCA1 decorates the unpaired X chromosome in human pachytene spermatocytes (Scully et al., 1997). To further evaluate this observation, we studied the localization of BRCA1 in sections of mouse testis. In pachytene cells, it decorated a specific curvilinear structure that is morphologically suggestive of the XY body. This was confirmed by costaining of BRCA1 in these structures with an antibody to macrohistone H2A1 (Figure 1C), a known XY body component (Richler et al., 2000). The XY body contains the unpaired X chromosome that has become densely heterochromatic, silenced, and localized at the nuclear periphery, much like the inactive X chromosome (Xi) in female somatic cells (Handel and Hunt, 1992; Huynh and Lee, 2001). Like Xi, the pachytene X is coated with the noncoding XIST RNA and accumulates macrohistone H2A1 (MH2A1), and its histone H3 is methylated on lysine 9 (Ayoub et al., 1997; Costanzi and Pehrson, 1998; Richler et al., 2000; Cowell et al., 2002).

Analysis of multiple female human cell lines and strains revealed that in a subset of unsynchronized cells, BRCA1 immunostaining colocalized with MH2A1 on a discrete nuclear structure (Figures 1D–1F). Concurrent immunostaining for BRCA1 and fluorescent in situ hybridization (FISH) for XIST RNA revealed significant colocalization of these signals in a subset of both WI-38 and telomerase-immortalized human mammary epithelial cells (HMEC-t) (Figures 1G–1L). Colocalization of BRCA1 and MH2A1 and BRCA1 and XIST on a large nuclear structure was detected in a subset of all lines/strains tested (see Figure 1 and Table 1). Since BRCA1 nuclear staining occurs primarily in S phase and MH2A1 staining of Xi can only be detected during late G1 and S (Chadwick and Willard, 2002), BRCA1/MH2A1 costaining was

not observed in all cells. Indeed, it varied from 4% to 12%, depending upon the cell line/strain analyzed (see Table 1). In keeping with these findings, colocalization was largely apparent in mid/late S phase cells (data not shown).

Coassociation of BRCA1 and BARD1 with XIST RNA

Chromatin immunoprecipitation (ChIP) analyses were performed on 293 cells using affinity-purified polyclonal BRCA1 antibodies. 293 cells are female, and the majority contain three X chromosomes, two of which are inactive (Gilbert et al., 2000). After ChIP, RNA was isolated and subjected to RT/PCR for XIST. A positive signal for XIST was observed in the anti-BRCA1 ChIP (Figure 1M). No such signal was detected in ChIPs generated with unrelated antibodies or when PCR was performed in the absence of a prior RT step (Figure 1M and data not shown). Similar results were obtained with extracts of WI-38 and with two monoclonal antibodies to BRCA1 (SD118 and SG11, data not shown). ChIP, performed with an antibody to BARD1, a structurally related protein that efficiently heterodimerizes with BRCA1, also coimmunoprecipitated XIST RNA (Figure 1M). By contrast, the same ChIPs lacked H19 RNA, another noncoding RNA (Figure 1N). These findings suggest that BRCA1 and BARD interact, directly or indirectly, with XIST RNA.

Although an XIST cDNA signal was reproducibly obtained from the ChIP when primers specific for a segment of the internal portion of XIST exon 6 were utilized, no such signal was detected when primers that flank the exon 1/2 junction or the exon 5/6 junction were used (Figure 1O), suggesting that BRCA1 and BARD1 associate with a specific segment(s) of XIST RNA.

Absence of XIST Staining in Human and Murine Tumor Cells that Lack Wild-Type BRCA1

To determine whether BRCA1 interacts functionally with Xi, we examined features of Xi in tumor cells that lack BRCA1. HCC1937 is a human breast cancer cell line that carries a germline mutation (5382insC) in one BRCA1 allele and has lost the wt allele (Tomlinson et

(N) ChIPs, performed on 293 cell extract, were subjected to RT-PCR using primers specific for H19 RNA.
(O) ChIP was performed as in (M), except that the relevant PCR primers spanned a region covering the XIST exon 1/2 junction (left) or a region spanning the Xist exon 5/6 junction (right).
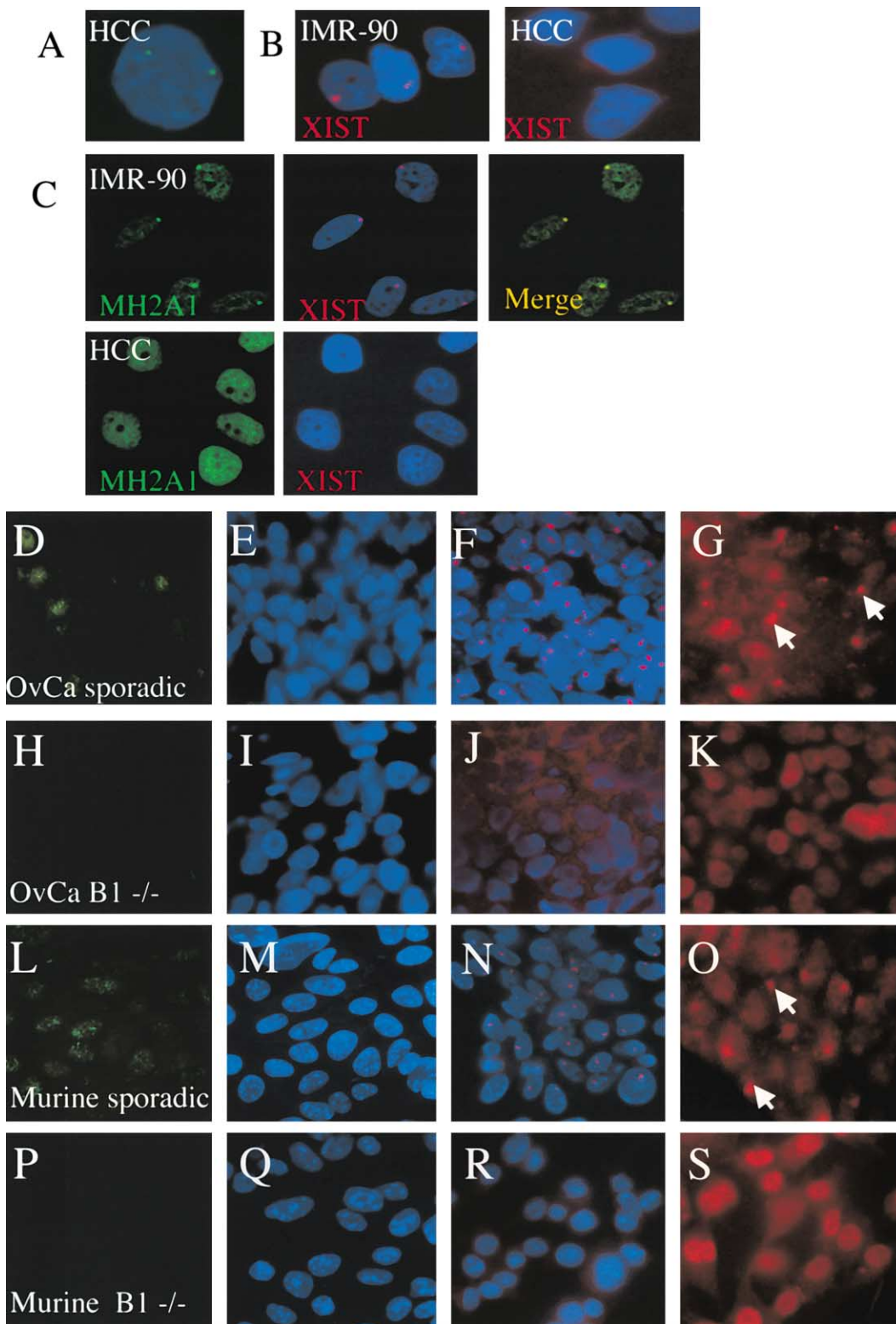
Figure 2. Absence of Focal XIST RNA and MH2A1 Staining in BRCA1$^{-/-}$ Cells

(A) DNA FISH using an X chromosome-specific probe was performed on HCC1937 cells. ~70% of the cells revealed two X foci. DAPI counterstaining is shown in blue.

(B) RNA FISH for XIST was performed on IMR-90 female diploid fibroblasts (left) and on HCC1937 cells (right). The FISH signal is in red; the DAPI nuclear staining is shown in blue. ~96% of IMR-90 revealed focal XIST staining, while none of the HCC cells contained a focal XIST signal.

(C) Simultaneous immunofluorescent (IF) staining for MH2A1 (left, green signal) and RNA FISH for XIST (middle, red signal; DAPI nuclear

Table 2. Correlation of BRCA1 Genotype and Focal XIST, MH2A1, and H3mK9 Localization in Breast and Ovarian Tumors

Tumor Type	B1 Genotype	BRCA1 IF	XIST	MH2A1	H3mK9
Human ovarian	sporadic	+	+	+	ND
Human ovarian	S713stop	−	−	−	ND
Human breast	sporadic	+	+	+	+
Human breast	sporadic	+	ND	ND	+
Human breast	sporadic	+	ND	ND	+
Human breast	C61G	−	−	−	−
Human breast	4476 ins G	−	−	−	−
Human breast	3448 del A	−	−	−	−[a]
Human breast	3600 del 11	−	−	−	−
Murine breast	wt	ND	+	+	ND
Murine breast	Del exon 11	ND	−	−	ND
Murine breast	Del exon 11	ND	−	−	ND

The generic nature of each tumor, its BRCA1 genotype (where known), and its BRCA1, XIST, MH2A1, and (where noted) histone H3mK9 staining characteristics are recorded for a series of human and murine tumors. Tissues were scored (−) for XIST and MH2A1 staining if <5% of malignant cells exhibited focal staining. IF for BRCA1 in murine breast tissue was not obtained (ND). All analyses were performed as described in Experimental Procedures.
[a] Small patches of focal, H3mK9-staining cells were detected in this sample against a much larger backdrop of negative staining cells in tumor-rich regions. The identities of the positive staining cells are not known.

al., 1998). These cells synthesize no wt BRCA1, although they do produce a mislocalized, truncated product (Scully et al., 1999). Most HCC1937 cells carry two X chromosomes (Figure 2A), although HCC are aneuploid and contain minor subpopulations of large cells bearing ≥6–8 X chromosomes (data not shown). Notably, nearly all HCC1937 cells, despite their ≥2 X chromosomal content, lacked focal XIST staining (Figure 2B). Unlike diploid female fibroblasts (IMR-90 or WI-38), they also lacked focal MH2A1 staining (Figure 2C). Loss of XIST and MH2A1 staining is not just a consequence of aneuploidy, since other aneuploid, female cancer cell lines (e.g., 293 and OVCAR3) maintain focal XIST and MH2A1/Xi staining (data not shown).

To determine whether the loss of focal XIST and MH2A1 staining is a consistent finding in BRCA1-deficient tumor cells, frozen sections of multiple human ovarian and breast cancers were analyzed. Sections from cases of sporadic breast and ovarian cancer revealed BRCA1 nuclear staining in a significant subset of tumor cells (Figures 2D and 2L and Table 2). Most cells also displayed focal XIST and MH2A1 staining (Figures 2F and 2G). However, when the four breast and one ovarian cancer arising in BRCA1^{+/−} women were analyzed, none revealed focal XIST or MH2A1 staining (compare Figures 2F and 2G with 2J and 2K, see also Table 2). The tumor cells in these samples all contained at least two X chromosomes (see Figure 6 and data not

shown). Although limited in quantity, these results reveal that the link between BRCA1 expression and XIST localization occurs in both cultured and primary BRCA1-deficient cells.

Similar findings were obtained with cell lines and frozen sections derived from BRCA1^{−/−} murine breast carcinomas (Figures 2R and 2S; Table 2; Brodie et al., 2001). By contrast, a cell line derived from a spontaneous murine mammary tumor and frozen sections of breast cancers from wt mice revealed BRCA1 nuclear immunostaining, focal Xist staining by RNA FISH, and focal macrohistoneH2A staining (Figures 2L–2O and Table 2).

Effect of Reconstituting HCC1937 with Wild-Type BRCA1
Stable reconstitution of HCC1937 cells with wt BRCA1 can be achieved by recombinant retroviral infection (Scully et al., 1999). The ectopically expressed protein is properly localized in nuclear foci and present at nearly physiological levels (Scully et al., 1999). Unlike the situation in HCC1937 cells transduced with vector alone, in which <1% of cells had detectable XIST staining, focal XIST staining was present in ≥65% of the BRCA1-reconstituted cells (Figures 3A and 3B). A few large cells contained several XIST-staining foci. Most likely, these cells carry multiple X chromosomes (data not shown).

Similar results were obtained during the analysis of an HCC1937 clone (HCC Clone5) that had been stably

staining is shown in blue) are shown for IMR-90 (top) and HCC1937 (bottom). Merged image of XIST and MH2A1 staining in IMR-90 is shown in the top right image. At least 200 cells of IMR-90 and HCC1937 were scored for MH2A1 staining, with 48% of IMR-90 and <1% of HCC cells showing a discrete nuclear focus of MH2A1.
(D–S) Human and mouse breast and/or ovarian tumor cells were subjected to IF staining for BRCA1 and MH2A1 and to FISH for XIST RNA. BRCA1 staining is shown for a frozen section of a sporadic ovarian cancer (D, with DAPI staining of the same section is shown in E). An adjacent frozen section was subjected to FISH for XIST RNA (F) and another to IF for MH2A1 (G; white arrows indicate typical MH2A1 focal staining structures). The one BRCA1^{−/−} ovarian tumor in the collection revealed no appreciable staining for BRCA1 (H, the DAPI image is in I) and no detectable focal XIST (J) or MH2A1 staining (K). Compared to that shown in (F), the red fluorescence channel gain in (J) was increased in an effort to detect low-level XIST staining. Spontaneous, 1687ARN mouse mammary tumor cells reveal focal nuclear staining for BRCA1 (L, with DAPI staining of these cells in M), focal Xist (N), and focal MH2A1 staining (O). W525 mouse mammary tumor cells that lack wt BRCA1 showed no detectable BRCA1 staining (P, with DAPI staining of these cells in Q), no focal Xist (R), and no focal MH2A1 staining (S). All the XIST staining is depicted in red with DAPI counterstaining of these nuclei in blue.
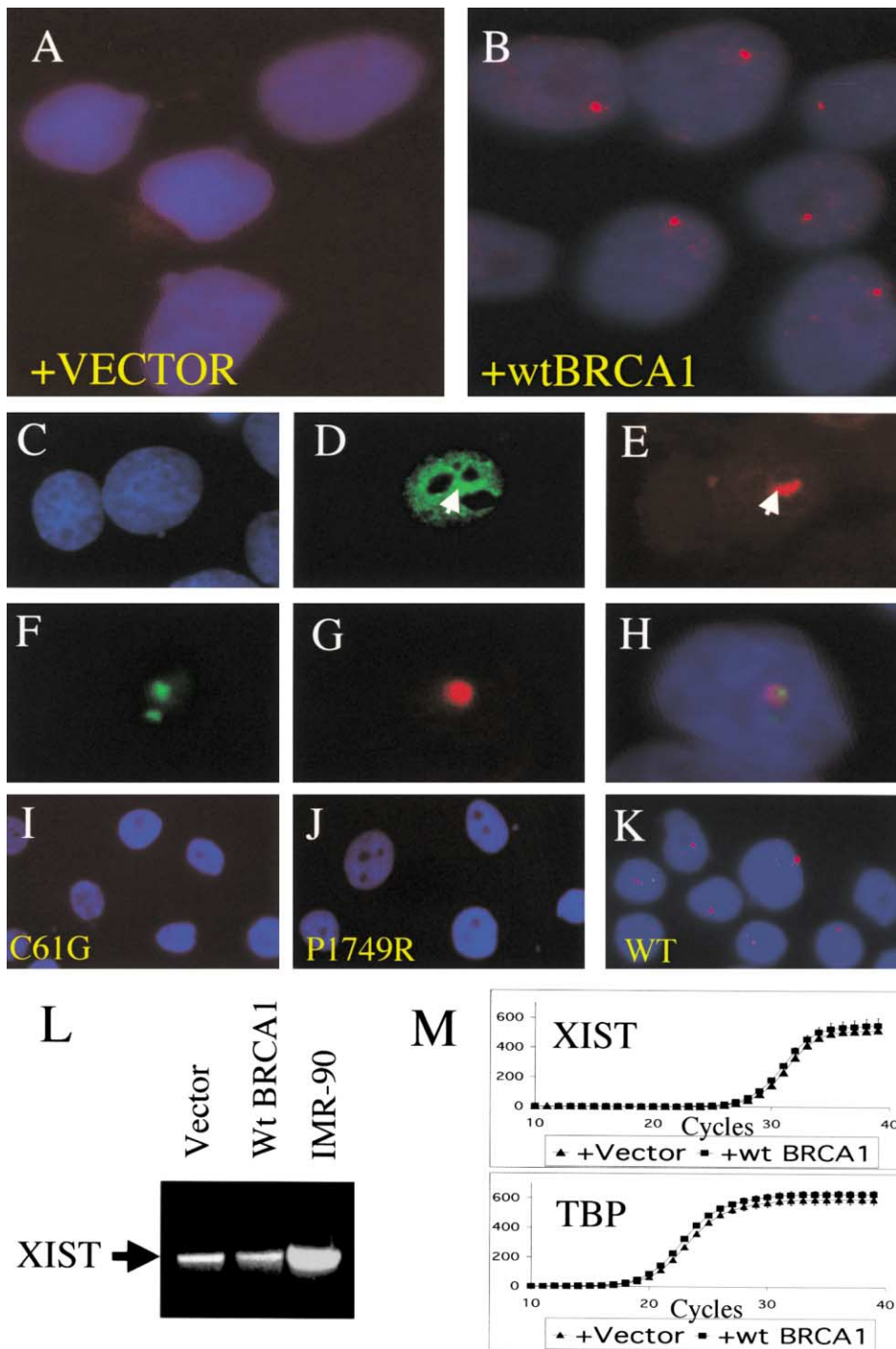
Figure 3. XIST RNA FISH Analysis of Naive and BRCA1-Reconstituted HCC1937 Cells

(A and B) XIST RNA FISH staining of vector-reconstituted HCC (A) or HCC that were stably reconstituted with wt BRCA1 (B).

(C–E) HCC stably transfected with a doxycycline-inducible wt BRCA1 vector (HCC Clone 5) were exposed to doxycycline for 24 hr. The cells were then paraformaldehyde fixed and subjected to combined immunostaining for BRCA1 (D) and RNA FISH for XIST (E). Nuclei were stained with DAPI (C). The arrow points to the region of greatest BRCA1 staining intensity, which coincides with the region that stains for XIST RNA.

(F–H) HCC Clone 5 were exposed to doxycycline to induce expression of BRCA1. DNA FISH for an X chromosome probe (F) and RNA FISH for XIST (G) were performed on the same cells. A merged image is shown in (H).

(I–K) RNA FISH for XIST (red) was performed in HCC stably reconstituted with either wt BRCA1 (K), or with vectors encoding clinically relevant BRCA1 mutant proteins bearing a missense mutations either in the RING domain, C61G (I), or in a BRCT domain, P1749R (J). DAPI staining of the nuclei is shown in blue.

(L) Total RNA was extracted from mock-reconstituted HCC1937 cells, from HCC cells reconstituted with wt BRCA1, and from naive IMR-90 and subjected to RT-PCR with primers specific for XIST RNA. The products were separated in 2% agarose gels and visualized by ethidium bromide staining.
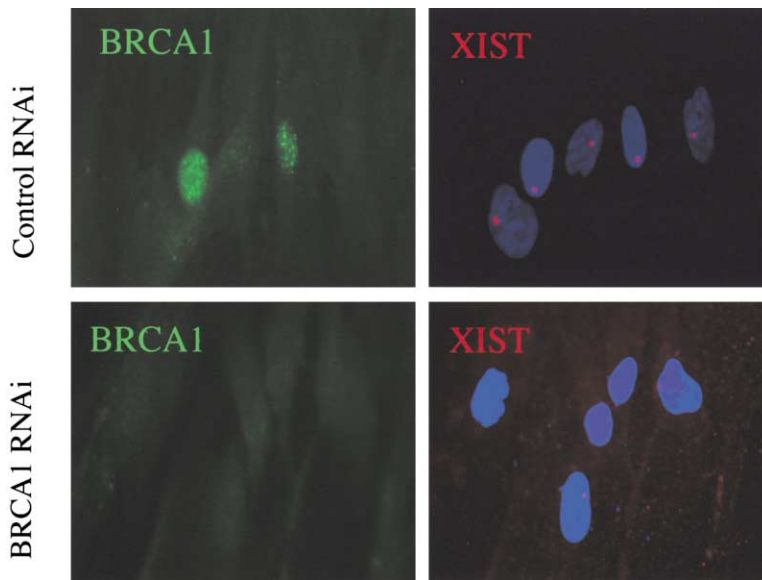
Figure 4. Effect of BRCA1 RNAi on XIST/Xi Staining

WI-38 were transfected with control siRNA (top) or with BRCA1-specific siRNA (bottom). After 72 hr, all cells were analyzed by immunostaining for BRCA1 (left) and by FISH for XIST RNA (right).

transfected with a doxycycline-inducible BRCA1 allele. Upon exposure to doxycycline, ~10% of the cells exhibited bright BRCA1 nuclear staining. Nearly all of these induced cells (~95%) also displayed focal nuclear accumulation of XIST RNA (Figures 3C–3E). Although immunostaining of the overexpressed BRCA1 was more diffuse than is normally the case for endogenous BRCA1 in other cell lines, the most intense staining typically concentrated over the XIST-bearing foci, suggesting that BRCA1 and XIST had colocalized therein (Figures 3D and 3E). Simultaneous X chromosomal DNA FISH and RNA FISH for XIST revealed that the XIST staining focus in these induced cells colocalized with one of the X chromosomes (Figures 3F–3H). Synthesis of either of two disease-associated BRCA1 mutant proteins failed to elicit focal XIST staining (Figures 3I–3K). Thus, intact BRCA1 appears to be required for focal XIST staining in this setting.

XIST RNA Levels in HCC1937 Cells

XIST RNA levels in vector- and wt BRCA1-reconstituted HCC1937 cells were compared by RT-PCR. Standard RT-PCR analyses revealed equivalent XIST RNA levels in these cells (Figure 3L). These results were confirmed by quantitative, real-time RT-PCR (Figure 3M). Similarly, there was no difference in XIST RNA levels in uninduced versus doxycycline-induced HCC Clone5 (data not shown). Therefore, introduction of wt BRCA1, although sufficient to induce widespread focal XIST staining in HCC1937, did not affect the XIST RNA level. Hence, in HCC1937 cells, BRCA1 does not affect either XIST RNA synthesis or stability. Instead, it appears to support XIST localization on Xi. In the absence of data from other cell lines/strains, a role for BRCA1 in the regulation of XIST

transcription or degradation in at least some cell types cannot be ruled out.

Effect of Suppressing BRCA1 Synthesis on XIST/Xi Costaining
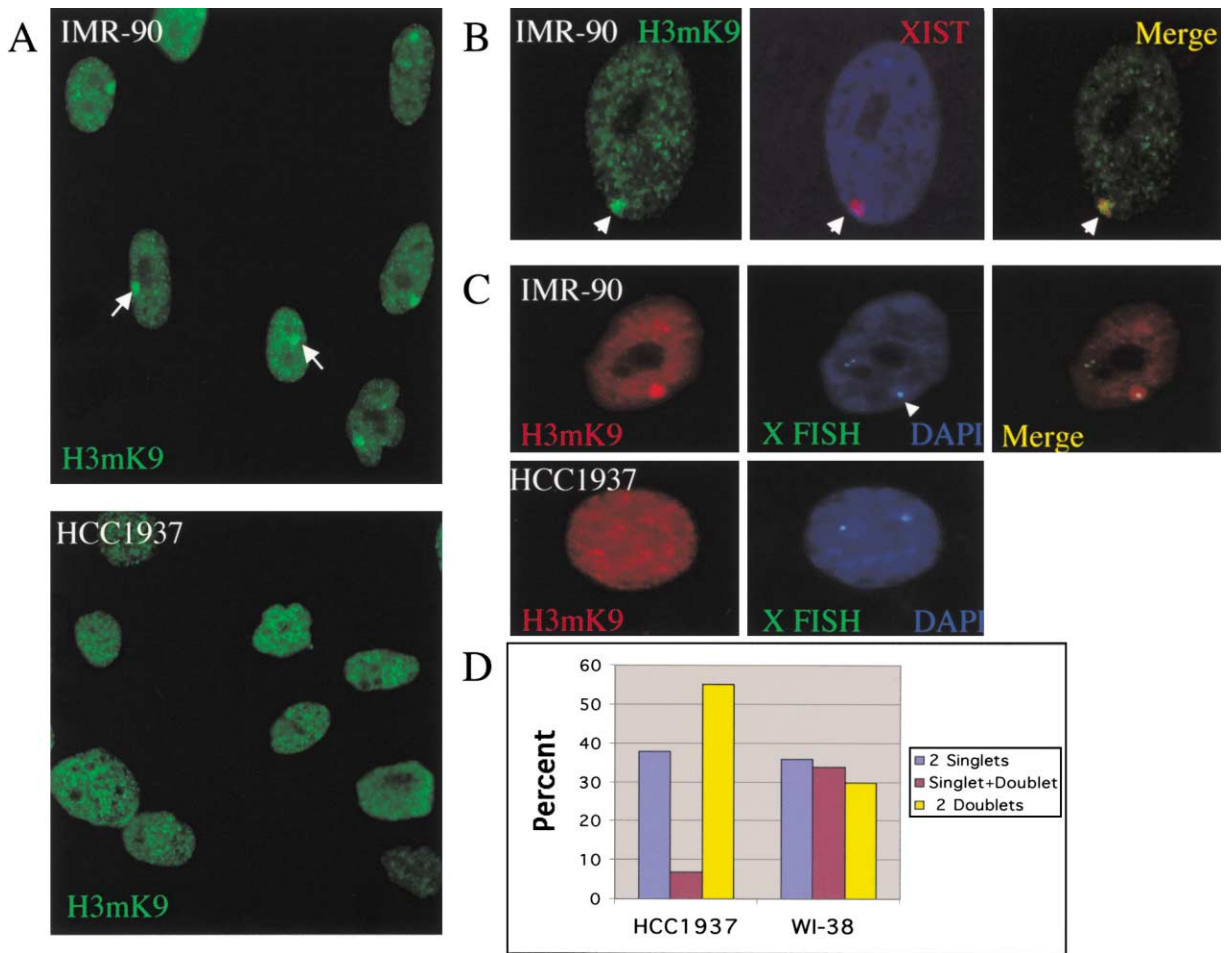
Small interfering RNA-mediated depletion (RNAi) specific for BRCA1 was employed to inhibit BRCA1 synthesis in cultured cells (Elbashir et al., 2001). Transfection of the diploid female strain, WI-38, with a BRCA1-specific RNAi, but not a control RNA, led to marked suppression of BRCA1 synthesis after 72 hr (Figure 4) and a marked decrease in focal XIST staining (Figure 4; 91% $\pm$ 2% of control cells revealed focal XIST staining versus 29% $\pm$ 10% of the BRCA1 RNAi-treated cells). Similar results were obtained in IMR-90 and in Ishikawa cells (endometrial cancer cells; data not shown). Thus, acute suppression of BRCA1 synthesis was associated with a significant loss of focal XIST staining.

Similarly, BRCA1 RNAi of asynchronous IMR-90 cells was associated with marked suppression of focal MH2A1 staining of Xi. No such effect was observed in control RNAi-treated cells analyzed in parallel (46% of control cells had focal MH2A1 staining, compared with 14% of BRCA1 RNAi-treated cells). Of note, RNAi-mediated suppression of BRCA2 synthesis did not lead to a change in focal XIST staining in IMR-90 (S.G., D.P.S., and D.M.L., unpublished results).

BRCA1-Deficient Tumor Cells Lack Focal Histone H3 Methylation on Lysine 9

The pattern of histone H3 methylation on lysine 9 (H3mK9) of the X chromosomes of BRCA1$^{+/+}$ versus BRCA1$^{-/-}$ cells was also assessed. H3/lys9 methylation occurs in certain transcriptionally silenced, heterochro-

---

(M) Total RNA from vector- and BRCA1-reconstituted HCC1937 was subjected to quantitative RT-PCR using primers specific for XIST or for TATA binding protein (TBP), an internal control. Fluorescence intensity is plotted versus cycle number. Each data point represents the mean and standard deviation of three measurements.

Figure 5. Histone H3 (Methyl) Lysine 9 Immunostaining and X Chromosome Replication Timing in a BRCA1-Deficient Cell Line

(A) IF for Histone H3 methylated at lysine 9 (H3mK9) is shown for IMR-90 (top) and HCC1937 (bottom). Most IMR-90 cells showed a discrete nuclear focus of H3mK9 staining, highlighted by the white arrows in two cells in the upper image. When more than 200 cells of each line were scored for H3mK9 focal staining, 53% of IMR-90 and <1% of HCC1937 were positive.

(B) IMR-90 underwent simultaneous immunostaining for H3mK9 (left, green) and RNA FISH for XIST (middle, red with DAPI nuclear staining in blue). Merged image (right; the overlapping signals are in yellow) demonstrates colocalization of the focal H3mK9 staining with the XIST staining, indicating that the area of focal H3mK9 staining is the Xi.

(C) Simultaneous immunostaining for H3mK9 (left, red) and X chromosomal DNA FISH (middle, grayish green with nuclear DAPI staining shown in blue) was performed on IMR-90 cells (top) and HCC1937 cells (bottom). A merged image of IMR-90 signals is shown in the upper right image. A singlet+doublet pattern of X chromosomal DNA FISH signals was observed for the IMR-90 cell that is depicted. The doublet signal seen in the upper part of the cell reflects replication of this X chromosome. The other X chromosome signal, highlighted by the white arrow, is a singlet, indicating that it has not yet replicated. This late-replicating X chromosome colocalized with the focus of H3mK9 staining in this cell. No unifocal H3mK9 staining was detected in the HCC1937 cell.

(D) HCC1937 cells and WI-38 female diploid fibroblasts were briefly labeled with BrdU and processed for both DNA FISH using an X chromosome-specific probe and for immunostaining for BrdU. The pattern of FISH staining seen in BrdU-positive cells was scored for at least 50 cells of each cell type. Cells with "two singlets" are cells in which neither X has yet replicated. Cells with a "singlet+doublet" pattern contain one unreplicated and one replicated X. In cells that contain "two doublets," both Xs have replicated.

matic regions (Lachner and Jenuwein, 2002). Moreover, in female cells there is a large concentration of H3mK9 on Xi (Figures 5A–5C; Heard et al., 2001; Peters et al., 2002). Although HCC1937 cells contain least two X chromosomes, they lack any focal H3mK9 staining (Figures 5A–5C). Replication timing analysis of the X chromosomes by FISH also showed that, unlike normal diploid fibroblasts, HCC1937 fail to demonstrate asynchronous replication of their X chromosomes (Figure 5D). These

observations point to a significant alteration in the chromatin structure of what would otherwise have been the Xi in these cells.

H3mK9 immunofluorescent staining was also performed on frozen sections of sporadic and BRCA1-deficient human breast cancers. As seen in Figure 6 and Table 2, tumor cells arising in a women with a germline mutation in BRCA1 lack focal H3mK9 staining, while bordering normal cells had intact staining. By contrast,
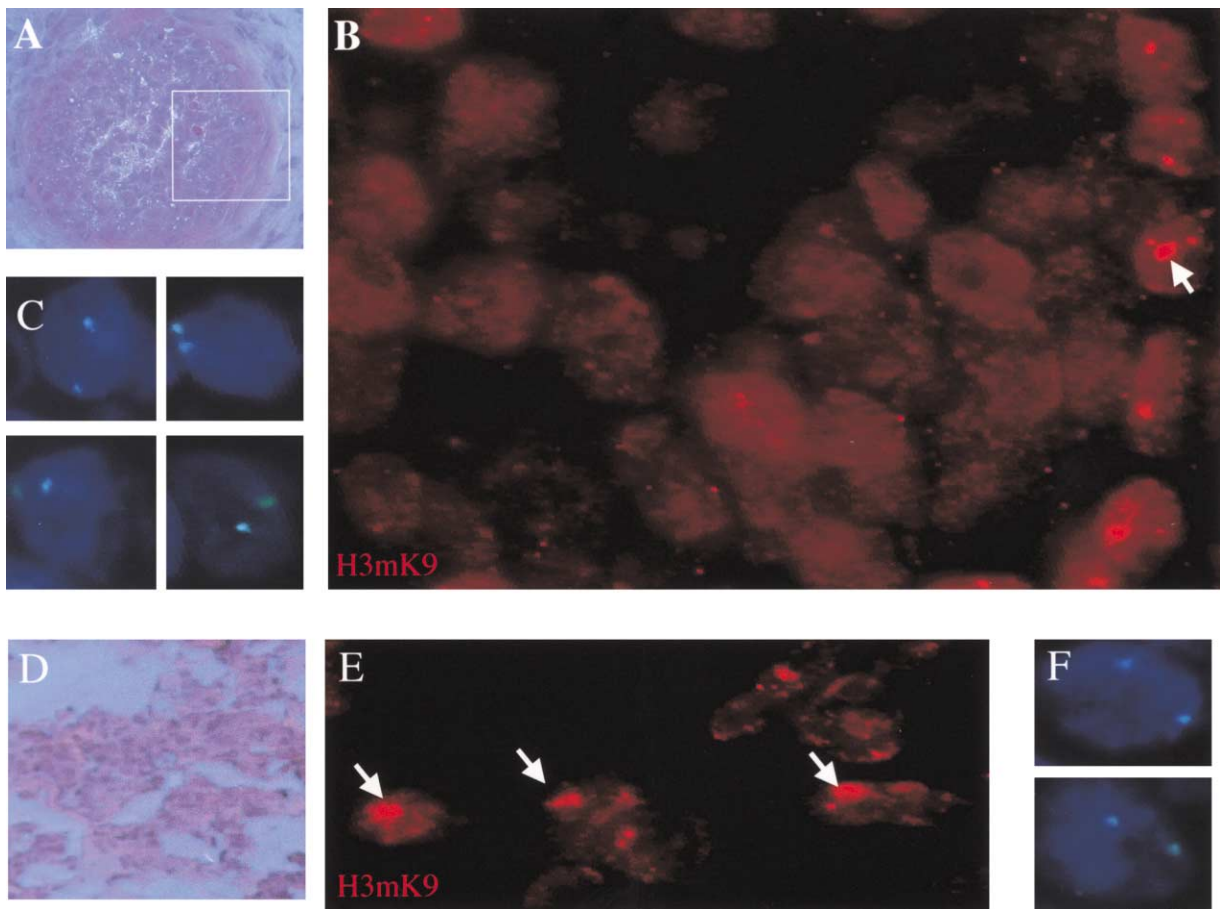
Figure 6. H3mK9 Immunostaining in Human Breast Cancer Tissue

(A) Hematoxylin and eosin (H & E)-stained, frozen section of a breast cancer arising in a woman with a germline BRCA1 mutation. The section contains a focus of tumor cells bounded by a ring of normal epithelial (and other) cells.

(B) The region highlighted with the white box in (A) was examined in higher power on an adjacent frozen section that was processed for IF using H3mK9 Ab. The normal cells at the periphery of this structure show clear unifocal nuclear staining (one focus is highlighted with a white arrow). However, the tumor cells within this cell boundary revealed no discrete staining (<5% of cells in malignant regions revealed focal nuclear staining when >200 cells from multiple regions of the tumor were analyzed). Similar results were obtained when frozen sections of two other breast cancers arising in women with germline BRCA1 mutations were stained for H3mK9 (see Table 2).

(C) DNA FISH using an X chromosome-specific probe was performed on an adjacent section of the same tumor shown in (A) and (B) with the FISH signal shown in green and DAPI nuclear staining in blue. Four representative tumor cells are shown, each revealing two X chromosomes.

(D) H & E staining of a sporadic breast cancer (this tumor revealed typical nuclear BRCA1 immunostaining, data not shown).

(E) High-power view of H3mK9 IF performed on an adjacent tumor section, demonstrating the staining of a focal nuclear structure in many of these cells (some examples are highlighted by a white arrow). When >200 cells were examined, 56% of cells in malignant regions of the frozen section revealed discrete nuclear H3mK9 foci.

(F) X chromosome-specific DNA FISH is shown for representative cells from this tumor.

focal H3mK9 staining was detected in tumor cells from sporadic, BRCA1-expressing breast cancers. Most cells of these tumors contain two X chromosomes (Figure 6).

**State of X Chromosome Gene Expression
in BRCA1-Depleted Cells**
To determine whether acute suppression of BRCA1 synthesis leads to a detectable change in Xi gene expression, we analyzed a female murine fibroblast cell line in which one X chromosome carries a nonfunctioning XIST allele and the other X expresses a wt XIST allele and carries a GFP transgene (similar to cells analyzed by Csankovszki et al. [2001]). The latter X chromosome is inactivated, and thus the GFP transgene is silenced. These cells were either mock-transfected, transfected with a control siRNA, transfected with a BRCA1-specific siRNA, or exposed to 5-azacytadine (AZC). AZC served as a positive control, leading to reactivated expression of the GFP allele in a fraction of cells of this and related cell lines (Csankovszki et al., 2001). These cultures were analyzed for GFP expression by FACS. As expected, by comparison with controls, treatment with AZC led to the appearance of GFP-positive cells (Figure 5B). The culture transfected with the BRCA1 RNAi also repeatedly displayed GFP-expressing cells (Figure 5B). The relative increase in GFP-expressing cells over back-
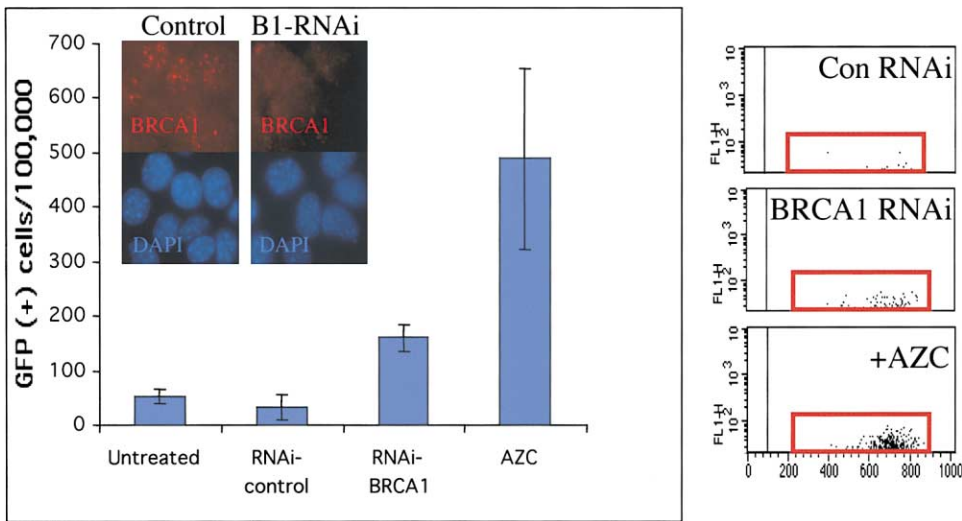
Figure 7. Effect of BRCA1 RNAi on Expression of an Xi GFP Transgene

A murine fibroblast line that carries a nonfunctional Xist allele on one X chromosome and a GFP transgene on the other was either mock-transfected, transfected with control RNAi, transfected with BRCA1-specific RNAi, or exposed to 5-azacytadine (AZC). After 72 hr, cells were analyzed by FACS for GFP expression. The number of cells gated GFP positive/100,000 cells is plotted for each condition. The mean and SE of at least three separate experiments are shown for each point. The inset figures depict the effect of BRCA1-specific RNAi on BRCA1 immunofluorescence in these cells. The figures on the right show a set of FACS profiles from one such experiment. The data are plotted as GFP fluorescence (y axis) versus forward scattering (x axis) of cells treated with control RNAi, BRCAi RNAi, or with AZC. For purposes of clarity, only data for cells that were gated positive (as determined by GFP fluorescence intensity and highlighted by the red box) are shown. The FACS profiles of the GFP-negative cells, which made up the vast majority of the cells in all conditions, were similar in all cases.

ground, both after AZC or BRCA1 RNAi treatment, although clearly incomplete, was similar in magnitude to the effect observed when the XIST gene was deleted from an analogous somatic murine cell line (Csankovszki et al., 2001).

Discussion

BRCA1 localizes, in part, on the inactive X chromosome both in pachytene spermatocytes and in female somatic cells. Moreover, it and its heterodimeric partner, BARD1, directly or indirectly interact with XIST RNA. Notably, BARD1 interacts with at least one protein engaged in RNA polyadenylation (Kleiman and Manley, 1999). Whether BARD1 and/or its associated protein(s) facilitates the BRCA1/XIST RNA interaction remains to be seen.

In both diploid female fibroblasts and established cell lines, a functional link between the synthesis of wt BRCA1 and the decoration of the inactive X with XIST RNA was apparent. Since, unlike the wt protein, two clinically relevant BRCA1 missense mutants failed to induce XIST staining in BRCA1$^{-/-}$ cells, it appears that intact BRCA1 function is needed for XIST staining of Xi.

No measurable difference in XIST RNA levels was observed between vector- and BRCA1-reconstituted HCC cells, although focal XIST staining on an X chromosome appeared in ≥65% of the latter. Thus, BRCA1 likely contributes to XIST/Xi localization, and one might hypothesize that its biochemical association with XIST contributes to this process. However, a role for BRCA1 in the regulation of transcription or degradation of XIST RNA in other cell types cannot be ruled out.

BRCA1 RNAi performed in human cells also led to specific suppression of macroH2A1 immunostaining of Xi. Therefore, acute loss of BRCA1 expression resulted in a significant change in both XIST localization on Xi and the associated histone composition of Xi. Taken together, these findings suggest that BRCA1 contributes to the continued association of Xi with certain key partner molecules that, in early embryonic cells, appear to contribute to the genesis of Xi. Whether BRCA1 participates in the initiation of X inactivation in the embryo is as yet unknown. These findings are also consistent with (although they do not prove) the hypothesis that BRCA1 dysfunction increases the risk of failure of the maintenance of X chromosome inactivation.

This hypothesis is supported by the finding that acute suppression of BRCA1 synthesis led to reproducible albeit inefficient expression of a formerly silenced GFP allele located on Xi. This result is consistent, both qualitatively and quantitatively, with results obtained by others (Csankovszki et al., 1999) who eliminated Xist RNA expression in a similar cell type and observed Xi gene activation in a small fraction of the culture. Whether the effect of BRCA1 loss on Xi silencing is completely due to the effect of BRCA1 loss on XIST localization is unclear. In principle, loss of BRCA1 may have other consequences, for example, compromise of genomic integrity control, that independently affect Xi structure and silencing.

HCC1937 cells lack focal staining of an X chromosome with XIST, MH2A1, and H3mK9, and both X chromosomes in these cells replicated synchronously. Thus, neither X in this established BRCA1$^{-/-}$ tumor cell line bears any of four established characteristics of Xi. Similarly, each member of a set of human BRCA1-deficient

breast carcinomas revealed no XIST, MH2A, and histone H3(me)lys9 staining of either X chromosome. By contrast, two sporadic, BRCA1-expressing carcinomas (one ovarian and one breast) revealed clear XIST and MH2A1 staining. In addition, the aforementioned breast cancer and one other sporadic, BRCA1-expressing breast carcinoma also revealed focal H3mK9 staining. These findings suggest a link between chronic BRCA1 loss and defects in multiple aspects of Xi chromatin structure.

If the absence of focal H3mK9 staining in BRCA1$^{-/-}$ tumor cells mirrors a major defect in Xi silencing, how might such a result fit with the relatively inefficient reactivation of an Xi gene observed after BRCA1 RNAi (see Figure 7)? One possibility is that complete and chronic absence of BRCA1 has a more powerful effect on Xi gene expression than its transient and incomplete depletion. Another is that additional genetic/epigenetic alterations beyond full BRCA1 loss might be needed to disrupt Xi silencing. In this regard, most BRCA1-deficient tumor cells are aneuploid, genomically unstable, contain multiple regions of LOH, bear p53 loss of function mutations, and likely harbor additional gene defects (Venkitaraman, 2002).

Multiple BRCA1$^{-/-}$ primary tumors exhibited defects in Xi chromatin structure, raising the question of whether these defects contribute to BRCA1-associated breast and ovarian tumorigenesis. This hypothesis is posed with the knowledge that X heterochromatinization and BRCA1 tumorigenesis are both female-specific events. Moreover, prior evidence supports a role for abnormal X chromosome behavior in breast and ovarian cancer. Notably, a subset of aggressive breast and ovarian carcinomas were shown to lack a detectable Barr body (Kimmel, 1957; Moore and Barr, 1957; Perry, 1972; Savino and Koss, 1971). Furthermore, compared to sporadic ovarian cancers, BRCA1-deficient ovarian cancers manifest overexpression of a set of X chromosomal genes (Jazaeri et al., 2002). However, it should be emphasized that, at present, there is no evidence to support a causal link between the effect of BRCA1 loss on Xi and tumor development.

The effect on Xi chromatin structure might be a reflection of a more general function of BRCA1. Perhaps the ability of BRCA1 to interact with XIST and to influence XIST/Xi localization is biochemically related to the execution of BRCA1 genomic integrity maintenance function. BRCA1 is not exclusively localized on the inactive X chromosome, even in female cells. Rather, during S phase, it also concentrates in another group of focal, nuclear structures (nuclear dots; Scully et al., 1997). Since the inactive X chromosome is a prominent form of facultative heterochromatin, it is possible that the nuclear dots are also heterochromatic elements. If so, perhaps BRCA1 participates in regulating the structure and function of certain heterochromatic structures after they have sustained DNA damage, thereby facilitating DNA repair.

Results presented here show that a RING domain protein (BRCA1) and a noncoding RNA dedicated to dosage compensation (XIST) communicate functionally in mammalian cells. Similar interactions between specific noncoding RNA molecules and a RING domain-containing protein participate in regulating sex chromosome dosage compensation through the control of chromatin structure in *Drosophila* (Kelley and Kuroda, 2000). There is also a role for RNA molecules in supporting the higher-order structure of pericentromeric heterochromatin (Maison et al., 2002). Thus, RNA plays a greater role in chromatin structure control than previously considered. Conceivably, the interaction of BRCA1 with XIST RNA is a reflection of a larger role for BRCA1 in influencing other aspects of chromatin structure control through specific RNA interactions.

Finally, there are families carrying germline loss of function BRCA1 mutations in which X inactivation is not random in affected family members (Buller et al., 1999). Further work will be required to learn whether these observations are related to the suggested participation of BRCA1 in the maintenance of Xi heterochromatin structure.

Experimental Procedures

Cells
HCC1937 cells and their BRCA1-reconstituted derivatives have been described previously (Scully et al., 1999). Ishikawa and telomerase-imortalized HMEC-t were a kind gift of Myles Brown. 1687ARN was a generous gift of Jing Yang and Robert Weinberg.

Antibodies
Monoclonal antibodies to mouse (GH118) and human BRCA1 (SD118, MS110, SG11) were used at a 1:10 dilution of hybridoma supernatant for immunofluorescence analyses. Affinity-purified polyclonal BRCA1 and BARD1 antibodies were described previously (Cantor et al., 2001; Chen et al., 1998). In immunofluorescence analyses, affinity-purified macroH2A1 antibody was used at a 1:500 dilution, anti-histone H3(me)lys9 antibody at a 1:500 dilution, and anti-BrdU (Becton Dickinson) at a 1:7 dilution.

Immunostaining
Immunostaining was performed on paraformaldehyde (PFA)-fixed cultured cells, as previously described (Scully et al., 1997). All samples were mounted with Vectashield containing DAPI (Vector Labs) prior to viewing.

Mouse testis sections from 2-month-old males mice were rapidly fixed in PBS and 3% PFA/PBS. They were then postfixed for 1 hr in 3% PFA/PBS and cryoprotected by O/N incubation in 20% sucrose at 4°C. 5–10 μm cryotome sections were then processed for immunostaining as described above.

RNA Fluorescence In Situ Hybridization (FISH)
Adherent, cultured cells or frozen sections of tumor samples were fixed in 3% PFA and then processed for RNA FISH as described (Clemson et al., 1996; Lee and Jaenisch, 1997). For combined immunostaining and RNA-FISH, samples were processed as described above for immunostaining, with RNAGuard (Amersham) added to all antibody incubations at a final concentration of 40 U/ml. After final washes, samples were refixed by incubation with 3% PFA/PBS for 20 min at 25 C. The samples were then processed for RNA-FISH as described above.

Interphase DNA FISH
Cells were fixed with paraformaldehyde, as described above. DNA FISH, using labeled X chromosome probe (XCEP, Vysis) or a FITC-labeled X chromosome paint (X-WCP, Vysis), was performed according to the manufacturer's instructions. For combined RNA+DNA FISH, samples were first processed for RNA-FISH as described above. After the final wash, the samples were crosslinked by incubation with 3% paraformaldehyde/PBS for 20 min at 24°C. Samples were then dehydrated with ethanol and processed for DNA FISH.

Replication Timing Analysis
Replication timing analysis for the X chromosome was performed as described (Squire et al., 2000).

Analysis of Frozen Tumor Sections

For immunostaining of tumor specimens, frozen sections were im-
mediately fixed by incubation with 3% PFA/PBS for 15 min at room
temperature. The fixed sections were processed for immunostaining
and RNA FISH as described above. Adjacent sections were stained
with hematoxylin and eosin and viewed to identify regions having
abundant malignant cells. ~200 malignant cells from each section
were assessed for the presence of focal XIST or MH2A1 staining.
Tumors were scored (−) for XIST, MH2A1, or H3mK9 focal nuclear
staining if <5% of the tumor cells analyzed were positive.

RT-PCR

RNA was isolated from cultured cells using Qiagen RNA-Mini kits
according to the manufacturer's instructions. For RNA analysis,
equivalent amounts of total RNA served as template for cDNA syn-
thesis using reverse-transcriptase, followed by PCR using specific
primers (Invitrogen, Superscript One-Step RT-PCR). PCR products
were separated in 2% Agarose gels and the resulting cDNA products
stained with ethidium bromide. For quantitative RT-PCR, Cybr-
Green (Molecular Probes) was added to the reaction mixture, and
fluorescence was measured after each cycle, using a BioRad
I-Cycler. Primers for TBP cDNA were used as internal normalization
controls (Bieche et al., 1999). The data are shown as mean and
standard deviation values of three measurements per data point.

Chromatin Immunoprecipitation

Cells were grown, harvested, washed in PBS, and crosslinked with
1% formaldehyde. Chromatin-IP was then performed essentially as
described (Shang et al., 2000). After reversal of crosslinking, nucleic
acids were purified from the eluate (Qiagen gel extraction kit) and
subjected to PCR either with or without first round RT performed
with specific primers. The primers used to detect XIST RNA were:
exon 6, sense 5′-CTTGAAGACCTGGGGAAATCCC and antisense 5′-
TGTCAATCTAAAGGTAACCGGC; exon 5/6 junction, sense 5′-GTG
CAGAGAGCTGAGTCTTCAGC and antisense 5′-GCAAAGGCACAC
ACGAAAGAAATTAGC; exon 1/2 junction, sense 5′- GCAAATAACTA
GTCATCACAACAGC and antisense 5′-CTAAGGACACATGCAGCG
TGG. H19 RNA: primers H3 and H4 were used as described (Squire
et al., 2000).

RNA Interference

Small interfering RNAs specific for BRCA1 were synthesized (Dhar-
macon) and transfected into WI-38 cells and Ishikawa cells using
Oligofectamine as described (Elbashir et al., 2001). After transfec-
tion, cells were harvested at 72 hr and processed for immunofluores-
cence and RNA FISH as described above. Cultures transfected un-
der otherwise identical conditions with an siRNA specific for
luciferase (Elbashir et al., 2001) regularly served as controls in these
experiments. The siRNA sequence used for human BRCA1 was
UCACAGUGUCCUUUAUGUA and that for murine BRCA1 was AAGG
GCCUUCACAAUGUCCUU.

Analysis of GFP Expression by FACS

Transformed mouse fibroblasts derived from embryos in which one
X chromosome contains a nonfunctional XIST gene and the other
carries a GFP transgene were generated as described (Csankovszki
et al., 2001). These cells were either mock transfected or transfected
with a control RNAi (luciferase), with an RNAi specific for murine
BRCA1, or exposed to 5-azacytadine (3 days at 300 nM). 72 hr after
transfection, the RNAi-treated cells were trypsinized to create a
single cell suspension, which was then fixed with 3% paraformalde-
hyde and subjected to FACS in search of a green fluorescing popula-
tion. Each analysis was performed with 100,000–200,000 cells. Each
data point depicted in the relevant figure represents the mean ±
SE of at least three independent experiments.

Acknowledgments

References

Ayoub, N., Richler, C., and Wahrman, J. (1997). Xist RNA is associ-
ated with the transcriptionally inactive XY body in mammalian male
meiosis. Chromosoma 106, 1–10.

Bieche, I., Onody, P., Laurendeau, I., Olivi, M., Vidaud, D., Lidereau,
R., and Vidaud, M. (1999). Real-time reverse transcription-PCR
assay for future management of ERBB2-based clinical applications.
Clin. Chem. 45, 1148–1156.

Blackshear, P.E., Goldsworthy, S.M., Foley, J.F., McAllister, K.A.,
Bennett, L.M., Collins, N.K., Bunch, D.O., Brown, P., Wiseman, R.W.,
and Davis, B.J. (1998). Brca1 and Brca2 expression patterns in mi-
totic and meiotic cells of mice. Oncogene 16, 61–68.

Bochar, D.A., Wang, L., Beniya, H., Kinev, A., Xue, Y., Lane, W.S.,
Wang, W., Kashanchi, F., and Shiekhattar, R. (2000). BRCA1 is asso-
ciated with a human SWI/SNF-related complex: linking chromatin
remodeling to breast cancer. Cell 102, 257–265.

Brodie, S.G., and Deng, C.X. (2001). BRCA1-associated tumorigene-
sis: what have we learned from knockout mice? Trends Genet. 17,
S18–22.

Brodie, S.G., Xu, X., Qiao, W., Li, W.M., Cao, L., and Deng, C.X.
(2001). Multiple genetic changes are associated with mammary tu-
morigenesis in Brca1 conditional knockout mice. Oncogene 20,
7514–7523.

Buller, R.E., Sood, A.K., Lallas, T., Buekers, T., and Skilling, J.S.
(1999). Association between nonrandom X-chromosome inactiva-
tion and BRCA1 mutation in germline DNA of patients with ovarian
cancer. J. Natl. Cancer Inst. 91, 339–346.

Cantor, S.B., Bell, D.W., Ganesan, S., Kass, E.M., Drapkin, R., Gross-
man, S., Wahrer, D.C., Sgroi, D.C., Lane, W.S., Haber, D.A., and
Livingston, D.M. (2001). BACH1, a novel helicase-like protein, inter-
acts directly with BRCA1 and contributes to its DNA repair function.
Cell 105, 149–160.

Chadwick, B.P., and Willard, H.F. (2002). Cell cycle-dependent local-
ization of macroH2A in chromatin of the inactive X chromosome. J.
Cell Biol. 157, 1113–1123.

Chen, J., Silver, D.P., Walpita, D., Cantor, S.B., Gazdar, A.F., Tomlin-
son, G., Couch, F.J., Weber, B.L., Ashley, T., Livingston, D.M., and
Scully, R. (1998). Stable interaction between the products of the
BRCA1 and BRCA2 tumor suppressor genes in mitotic and meiotic
cells. Mol. Cell 2, 317–328.

Clemson, C.M., McNeil, J.A., Willard, H.F., and Lawrence, J.B. (1996).
XIST RNA paints the inactive X chromosome at interphase: evidence
for a novel RNA involved in nuclear/chromosome structure. J. Cell
Biol. 132, 259–275.

Costanzi, C., and Pehrson, J.R. (1998). Histone macroH2A1 is con-
centrated in the inactive X chromosome of female mammals. Nature
393, 599–601.

Cowell, I.G., Aucott, R., Mahadevaiah, S.K., Burgoyne, P.S., Huskis-
son, N., Bongiorni, S., Prantera, G., Fanti, L., Pimpinelli, S., Wu, R.,
et al. (2002). Heterochromatin, HP1 and methylation at lysine 9 of
histone H3 in animals. Chromosoma 111, 22–36.

Csankovszki, G., Panning, B., Bates, B., Pehrson, J.R., and Jaenisch,
R. (1999). Conditional deletion of Xist disrupts histone macroH2A
localization but not maintenance of X inactivation. Nat. Genet. 22,
323–324.

Csankovszki, G., Nagy, A., and Jaenisch, R. (2001). Synergism of Xist

RNA, DNA methylation, and histone hypoacetylation in maintaining X chromosome inactivation. J. Cell Biol. *153*, 773–784.

Deng, C.X., and Brodie, S.G. (2000). Roles of BRCA1 and its interacting proteins. Bioessays *22*, 728–737.

Elbashir, S.M., Harborth, J., Lendeckel, W., Yalcin, A., Weber, K., and Tuschl, T. (2001). Duplexes of 21-nucleotide RNAs mediate RNA interference in cultured mammalian cells. Nature *411*, 494–498.

Fan, S., Ma, Y.X., Wang, C., Yuan, R.Q., Meng, Q., Wang, J.A., Erdos, M., Goldberg, I.D., Webb, P., Kushner, P.J., et al. (2001). Role of direct interaction in BRCA1 inhibition of estrogen receptor activity. Oncogene *20*, 77–87.

Garcia-Higuera, I., Taniguchi, T., Ganesan, S., Meyn, M.S., Timmers, C., Hejna, J., Grompe, M., and D'Andrea, A.D. (2001). Interaction of the Fanconi anemia proteins and BRCA1 in a common pathway. Mol. Cell *7*, 249–262.

Gilbert, S.L., Pehrson, J.R., and Sharp, P.A. (2000). XIST RNA associates with specific regions of the inactive X chromatin. J. Biol. Chem. *275*, 36491–36494.

Gowen, L.C., Avrutskaya, A.V., Latour, A.M., Koller, B.H., and Leadon, S.A. (1998). BRCA1 required for transcription-coupled repair of oxidative DNA damage. Science *281*, 1009–1012.

Handel, M.A., and Hunt, P.A. (1992). Sex-chromosome pairing and activity during mammalian meiosis. Bioessays *14*, 817–822.

Hashizume, R., Fukuda, M., Maeda, I., Nishikawa, H., Oyake, D., Yabuki, Y., Ogata, H., and Ohta, T. (2001). The RING heterodimer BRCA1-BARD1 is a ubiquitin ligase inactivated by a breast cancer-derived mutation. J. Biol. Chem. *276*, 14537–14540.

Heard, E., Rougeulle, C., Arnaud, D., Avner, P., Allis, C.D., and Spector, D.L. (2001). Methylation of histone H3 at Lys-9 is an early mark on the X chromosome during X inactivation. Cell *107*, 727–738.

Huynh, K.D., and Lee, J.T. (2001). Imprinted X inactivation in eutherians: a model of gametic execution and zygotic relaxation. Curr. Opin. Cell Biol. *13*, 690–697.

Jazaeri, A.A., Yee, C.J., Sotiriou, C., Brantley, K.R., Boyd, J., and Liu, E.T. (2002). Gene expression profiles of BRCA-linked and sporadic ovarian cancers. J. Natl. Cancer Inst. *94*, 990–1000.

Kelley, R.L., and Kuroda, M.I. (2000). Noncoding RNA genes in dosage compensation and imprinting. Cell *103*, 9–12.

Kimmel, V.M. (1957). Clinical-cytological correlations of mammary carcinoma based upon sex-chromatin counts. Cancer *10*, 922–927.

Kleiman, F.E., and Manley, J.L. (1999). Functional interaction of BRCA1-associated BARD1 with polyadenylation factor CstF-50. Science *285*, 1576–1579.

Lachner, M., and Jenuwein, T. (2002). The many faces of histone lysine methylation. Curr. Opin. Cell Biol. *14*, 286–298.

Lee, J.T., and Jaenisch, R. (1997). Long-range cis effects of ectopic X-inactivation centres on a mouse autosome. Nature *386*, 275–279.

Maison, C., Bailly, D., Peters, A.H., Quivy, J.P., Roche, D., Taddei, A., Lachner, M., Jenuwein, T., and Almouzni, G. (2002). Higher-order structure in pericentric heterochromatin involves a distinct pattern of histone modification and an RNA component. Nat. Genet. *19*, 329–334.

Moore, R., and Barr, M. (1957). The sex chromatin in human malignant tissues. Br. J. Cancer *11*, 384–390.

Moynahan, M.E., Chiu, J.W., Koller, B.H., and Jasin, M. (1999). Brca1 controls homology-directed DNA repair. Mol. Cell *4*, 511–518.

Paull, T.T., Cortez, D., Bowers, B., Elledge, S.J., and Gellert, M. (2001). From the cover: direct DNA binding by Brca1. Proc. Natl. Acad. Sci. USA *98*, 6086–6091.

Perry, M. (1972). Evaluation of breast tumour sex chromatin (Barr body) as an index of survival and response to pituitary ablation. Br. J. Surg. *59*, 731–734.

Peters, A.H., Mermoud, J.E., O'Carroll, D., Pagani, M., Schweizer, D., Brockdorff, N., and Jenuwein, T. (2002). Histone H3 lysine 9 methylation is an epigenetic imprint of facultative heterochromatin. Nat. Genet. *30*, 77–80.

Richler, C., Soreq, H., and Wahrman, J. (1992). X inactivation in mammalian testis is correlated with inactive X-specific transcription. Nat. Genet. *2*, 192–195.

Richler, C., Dhara, S.K., and Wahrman, J. (2000). Histone macroH2A1 is concentrated in the XY compartment of mammalian male meiotic nuclei. Cytogenet. Cell Genet. *89*, 118–120.

Savino, A., and Koss, L.G. (1971). The evaluation of sex chromatin as a prognostic factor in carcinoma of the breast. A preliminary report. Acta Cytol. *15*, 372–374.

Scully, R., and Livingston, D.M. (2000). In search of the tumour-suppressor functions of BRCA1 and BRCA2. Nature *408*, 429–432.

Scully, R., Chen, J., Plug, A., Xiao, Y., Weaver, D., Feunteun, J., Ashley, T., and Livingston, D.M. (1997). Association of BRCA1 with Rad51 in mitotic and meiotic cells. Cell *88*, 265–275.

Scully, R., Ganesan, S., Vlasakova, K., Chen, J., Socolovsky, M., and Livingston, D.M. (1999). Genetic analysis of BRCA1 function in a defined tumor cell line. Mol. Cell *4*, 1093–1099.

Shang, Y., Hu, X., DiRenzo, J., Lazar, M.A., and Brown, M. (2000). Cofactor dynamics and sufficiency in estrogen receptor-regulated transcription. Cell *103*, 843–852.

Squire, J.A., Li, M., Perlikowski, S., Fei, Y.L., Bayani, J., Zhang, Z.M., and Weksberg, R. (2000). Alterations of H19 imprinting and IGF2 replication timing are infrequent in Beckwith-Wiedemann syndrome. Genomics *65*, 234–242.

Tomlinson, G.E., Chen, T.T., Stastny, V.A., Virmani, A.K., Spillman, M.A., Tonk, V., Blum, J.L., Schneider, N.R., Wistuba, I.I., Shay, J.W., et al. (1998). Characterization of a breast cancer cell line derived from a germ-line BRCA1 mutation carrier. Cancer Res. *58*, 3237–3242.

Venkitaraman, A.R. (2002). Cancer susceptibility and the functions of BRCA1 and BRCA2. Cell *108*, 171–182.

Wang, Y., Cortez, D., Yazdi, P., Neff, N., Elledge, S.J., and Qin, J. (2000). BASC, a super complex of BRCA1-associated proteins involved in the recognition and repair of aberrant DNA structures. Genes Dev. *14*, 927–939.

Xu, X., Wagner, K.U., Larson, D., Weaver, Z., Li, C., Ried, T., Hennighausen, L., Wynshaw-Boris, A., and Deng, C.X. (1999). Conditional mutation of Brca1 in mammary epithelial cells results in blunted ductal morphogenesis and tumour formation. Nat. Genet. *22*, 37–43.

Zheng, L., Pan, H., Li, S., Flesken-Nikitin, A., Chen, P.L., Boyer, T.G., and Lee, W.H. (2000). Sequence-specific transcriptional corepressor function for BRCA1 through a novel zinc finger protein, ZBRK1. Mol. Cell *6*, 757–768.

Zheng, L., Annab, L.A., Afshari, C.A., Lee, W.H., and Boyer, T.G. (2001). BRCA1 mediates ligand-independent transcriptional repression of the estrogen receptor. Proc. Natl. Acad. Sci. USA *98*, 9587–9592.

Zhong, Q., Chen, C.F., Li, S., Chen, Y., Wang, C.C., Xiao, J., Chen, P.L., Sharp, Z.D., and Lee, W.H. (1999). Association of BRCA1 with the hRad50-hMre11-p95 complex and the DNA damage response. Science *285*, 747–750.